

Supplementary Appendix

This appendix has been provided by the authors to give readers additional information about their work.

Supplement to: Moretti A, Bellin M, Welling A, et al. Patient-specific induced pluripotent stem-cell models for long-QT syndrome. *N Engl J Med* 2010;363:1397-1409. DOI: [10.1056/NEJMoa0908679](https://doi.org/10.1056/NEJMoa0908679).

Supplementary Appendix

Content

- 1. Supplementary Methods, Results, and Discussion**
- 2. Supplementary Tables**
- 3. Supplementary Figures**
- 4. Supplementary Movie Legends**
- 5. Supplementary References**

1. Supplementary Methods, Results, and Discussion

Methods

Individuals involved in the study

Under human research subject protocols approved by the institutional review boards and the ethic committee of both the Klinikum rechts der Isar and the Technical University of Munich, we recruited the father and son in the family affected by long-QT syndrome type 1 (LQT1) and two healthy control subjects to be used in reprogramming studies. The control subjects were 32 and 36 year old Caucasian female patients attending the hospital for plastic surgical interventions. Both individuals had a normal health status without a history of cardiac disease or any cardiovascular risk factors.

Cell culture

Dermal fibroblasts from LQT1 patients and healthy controls were obtained from skin biopsies, which were minced into 2 mm pieces, placed on culture dishes, and incubated in Quantum 333 medium (PAA). Cells migrating out of the explants were passaged in DMEM containing 10% FBS and used at passage 3 for induced pluripotent stem cell (iPSC) generation.

After derivation, iPSCs were grown on murine embryonic fibroblast (MEF) feeders in human embryonic stem cell (ESC) medium consisting of DMEM/F12 supplemented with 20% knockout

serum replacement (KSR, Invitrogen), 2 mM L-glutamine, 0.1 mM nonessential amino acids, 0.1 mM β -mercaptoethanol, 50 U/ml penicillin, 50 μ g/ml streptomycin and 10 ng/ml human b-FGF (R&D).

H9c2 and HEK293T cells were cultured in DMEM containing 10% FBS, 2 mM L-glutamine, 50 U/ml penicillin, and 50 μ g/ml streptomycin.

Retrovirus production and iPSC induction

Retroviruses were produced in HEK293T cells that were independently transfected with one of the pMXs-based retroviral vectors for the human *OCT3/4*, *SOX2*, *KLF4*, and *c-MYC* (Addgene plasmids 17217, 17218, 17219, and 17220) and the combination of moloney gag-pol plasmid pUMVC (Addgene plasmid 8449) and VSV envelope plasmid (Addgene plasmid 8454) in DMEM containing 10% FBS using Fugene HD (Roche). Viral supernatants were harvested after 48 h, filtered through a 0.45 μ m low protein binding cellulose acetate filter, concentrated by spin column (Millipore) and used directly to infect 1.6×10^5 human fibroblasts in the presence of 8 μ g/ml polybrene. Infection was repeated 24 h later. The medium was changed 24 and 72 h after the second infection and infected cells were seeded on MEF feeders at a density of 25×10^3 cells per 10 cm dish on day 4 after the second infection. After 3-4 additional weeks of culture in human ESC medium, colonies were manually picked based on their morphological similarity to human ESCs.

Embryoid body (EB) formation and cardiac differentiation

Control and patient iPSCs were differentiated as EBs by detaching iPSC colonies from MEF feeders using PBS containing 2.5 mg/ml trypsin (USB), 1 mg/ml collagenase IV (Invitrogen), 20% KSR, and 1 mM CaCl_2 (5 min at 37 $^\circ\text{C}$) and maintaining them for 3 days in MEF-conditioned human ESC medium in low attachment plates coated with 5% (w/vol) poly-HEMA (Sigma-Aldrich). For spontaneous differentiation, medium was then replaced with DMEM/F12 supplemented with 20% FBS, 2 mM L-glutamine, 0.1 mM nonessential amino acids, 0.1 mM β -mercaptoethanol, 50 U/ml penicillin, and 50 μ g/ml streptomycin. To improve cardiac

differentiation, ascorbic acid (50 µg/ml) was added to the medium and EBs were plated on day 7 on gelatin-coated dishes for better detection of beating foci. At day 20-30 of EB differentiation, contracting areas were manually micro-dissected and plated on fibronectin-coated plates. These myocytic explants were maintained in culture in the same medium described for EB differentiation, but supplemented with 2% FBS.

For single-cell analysis, myocytic explants were dissociated with several rounds of 15 min incubation at 37 °C with 480 U/ml collagenase type II (Worthington) under gentle shaking. Dissociated cells were plated on fibronectin-coated plastic cover slides for immunohistochemical analysis and electrophysiological measurements.

Genomic sequencing

Genomic DNA was isolated from control and patient dermal fibroblasts and iPSCs using Genomic DNA Purification Kit (Gentra Systems). PCR reactions were performed using 50 ng of genomic DNA with primers corresponding to the mutated region located in exon 2 of the *KCNQ1* gene. Primer sequences are provided in Supplementary Table 1. PCR products were then sequenced (Eurofins MWG Operon).

Quantitative real-time PCR (qRT-PCR) and reverse transcription PCR (RT-PCR)

Total mRNA was isolated from fibroblasts, iPSC clones, EBs, and myocytic explants using the Stratagene Absolutely RNA kit and 1 µg was used to synthesize cDNA using the High-Capacity cDNA Reverse Transcription kit (Applied Biosystems). Gene expression was quantified by qRT-PCR using 1 µl of the RT reaction and the Power SYBR Green PCR Master Mix (Applied Biosystems). Gene expression levels were normalized to *GAPDH*. Single-cell RT-PCR was performed after electrophysiological recording by harvesting the same cell using a second patch-clamp pipette. The content was expelled into a tube containing the RT reaction mixture (High-Capacity Reverse Transcription kit, Applied Biosystems). Reverse transcription was performed

immediately, in a final volume of 10 μ l and PCR was carried out using 1 μ l of the RT reaction. A list of the primers is provided in Supplementary Table 1.

***KCNQ1-569G* and *KCNQ1-569A* allelic discrimination**

The primers and probes used in qRT-PCR to detect the wild-type *KCNQ1* (569G) and the mutated *KCNQ1* (569A) alleles were obtained from Applied Biosystems Custom TaqMan SNP Assay service. RNA from control and LQT1 myocytic explants was purified and reverse transcribed as described above. One μ l of the RT reaction was used for each qRT-PCR reaction.

In order to establish a *KCNQ1* allelic standard curve, the specific mutation 569G>A was introduced into the wild-type pCI-*KCNQ1* construct using the QuickChange XL Site-Directed Mutagenesis Kit (Stratagene). The coding regions of the wild-type and mutated *KCNQ1* were amplified and mixed at the following ratios: 8:1, 4:1, 2:1, 1:1, 1:2, 1:4, and 1:8 (*KCNQ1*-569G allele:*KCNQ1*-569A allele)¹.

Immunohistological analysis and alkaline phosphatase activity detection

Cells and EBs were fixed with 3.7% (vol/vol) formaldehyde and subjected to immunostaining by using the following primary antibodies: human Nanog (rabbit polyclonal, Abcam, 1:500), TRA1-81-Alexa-Fluor-488-conjugated (mouse monoclonal, BD Pharmingen, 1:20), cardiac troponin T (mouse monoclonal clone 13-11, Lab Vision, 0.4 μ g/ml), α -actinin (mouse monoclonal clone EA-53, Sigma-Aldrich, 1:300), myosin light chain 2v (mouse monoclonal clone 33045, Synaptic Systems, 1:200), myosin light chain 2a (unconjugated and ATTO-647-labeled mouse monoclonal clone 56F5, Synaptic Systems, 1:200), *KCNQ1* (rabbit polyclonal, Abcam, 1:100), and protein disulfide isomerase (mouse monoclonal clone RL-90, Abcam 1:100). Alexa-Fluor-488, -594, and -647 conjugated secondary antibodies specific to the appropriate species were used (Invitrogen, 1:500). Phalloidin-Alexa-Fluor-594-conjugated (Invitrogen, 1:40) was used to stain F-actin. Nuclei were detected with 1 μ g/ml Hoechst 33528. Direct alkaline phosphatase activity was analyzed using

the NBT/BCIP alkaline phosphatase blue substrate (Roche), according to the manufacturer's guidelines.

Microscopy was performed using imaging systems (DMI6000-AF6000 and TCS SP5), filter cubes and software from Leica microsystems. Images were assigned with pseudo-colors and processed using Image J software (NIH).

Western blotting

Western blotting was performed using standard protocols, with the following antibodies: KCNQ1 (rabbit polyclonal, Abcam, 1:100) and β -actin (mouse monoclonal, Abcam, 1:5000).

Electrophysiology

Electrophysiological recordings were obtained in the current-clamp and voltage-clamp mode of the whole-cell patch-clamp technique² with an EPC9 amplifier (HEKA Electronics, Lambrecht/Pfalz, Germany). The sampling rate was 2 kHz for current recordings or 0.5-10 kHz for voltage recordings. Culture differentiation medium was used as external bath solution and contained 120 mM NaCl, 4.2 mM KCl, 0.4 mM MgSO₄, 0.5 mM Na₂HPO₄, 0.3 mM MgCl₂, 1 mM CaCl₂, 10 mM HEPES, 29 mM NaHCO₃, and 17.5 mM glucose, pH 7.4. The pipette resistances were 3 to 4 M Ω when filled with 120 mM K-Aspartate, 25 mM KCl, 1 mM MgCl₂, 1 mM CaCl₂, 10 mM EGTA, 5 mM HEPES, 4 mM Na₂-ATP, 2 mM Na₂-Phosphocreatine, 2.2 mM Na-GTP, pH adjusted to 7.2 with KOH. Capacitance and 60-80% of series resistance were routinely compensated. Action potentials and currents were recorded at approximately 35 °C. Only spontaneously beating cells were measured. Chromanol 293B (10 μ M, TOCRIS) and E-4031 (1 μ M, TOCRIS) were used in the external solution to isolate I_{Ks} and I_{Kr} currents, respectively. Isoproterenol (100 nM), adrenaline (1 μ M), and propranolol (200 nM) were purchased from Sigma-Aldrich. All currents were normalized to cell capacitance determined using Pulse (HEKA). No leak subtraction was applied.

All cells analyzed electrophysiologically for the different experiments have been included in the evaluation of the results, with the exception of cells displaying an early immature action potential electrophysiological phenotype and cells unable to respond to pacing.

Electrophysiological recordings were performed by investigators blinded to the genotype of the cells.

Heterologous expression and imaging of fluorescent KCNQ1 fusion proteins

The cDNAs of human wild-type KCNQ1 and R190Q-KCNQ1 were subcloned into pCI expression vectors and in-frame into N-terminal cyan fluorescent protein (CFP) and yellow fluorescent protein (YFP) fusion expression vectors³. The construct of β_1 -receptor fused with a yellow fluorescent protein (YFP- β_1 -R) was a generous gift of Andrea Ahles. H9c2 and HEK293T cells were transiently transfected with these plasmids and a KCNE1 expression vector using Fugene HD (Roche) transfection reagent according to the manufacturer's instructions.

For simultaneous imaging of CFP and YFP fluorescence, pairs of fluorescence images were acquired using specific filter sets (excitation bandpass 436/20 nm, beamsplitter 455 nm, emission bandpass 480/40 nm for CFP; excitation bandpass 495/14 nm, beamsplitter 510 nm, emission bandpass 530/30 nm for YFP). Exposure times between 10 and 100 ms were used. Fluorescence resonance energy transfer (FRET) was measured by an acceptor photobleaching approach as described³. Six pairs of CFP and YFP fluorescence images were acquired, alternating with 30 s pulses of illumination using the YFP filter set to photobleach the YFP. For each fluorescent cell, a region of interest (ROI) containing the whole fluorescent area as well as a corresponding background ROI over a cell that escaped transfection was defined. The background-corrected fluorescence intensities of CFP and YFP were used to linearly extrapolate the CFP fluorescence intensity in the absence of any YFP to calculate the FRET efficiency³.

Modeling of the KCNQ1 subunit composition

Assuming that a pore-forming KCNQ1 channel complex consists of a tetramer composed of wild-type (w) or mutant (m) KCNQ1 subunits, 5 different types of tetramers can be formed: wwww, wwvm, wvmm, mmmm. Assuming that the mutation does not alter the ability of the mutated subunit to co-assemble with other subunits, the distribution of the different types of tetramers is only dependent on the ratio between available w and m subunits: for a given proportion of w subunits $P(w)$, with $P(w)$ ranging from 0 to 1 and the proportion of m subunits $P(m)$ calculated as $1 - P(w)$, the proportion of the different tetramers can be calculated as

$$P(wwww) = P(w) \times P(w) \times P(w) \times P(w)$$

$$P(wwvm) = 4 \times P(w) \times P(w) \times P(w) \times P(m)$$

$$P(wvmm) = 6 \times P(w) \times P(w) \times P(m) \times P(m)$$

$$P(mmmm) = 4 \times P(w) \times P(m) \times P(m) \times P(m)$$

$$P(mmmm) = P(m) \times P(m) \times P(m) \times P(m)$$

For Figure 3C, the fraction of functional channels $F(\text{funct})$ was plotted as a function of $P(m)$ assuming 4 different models:

(1) The presence of 1 m subunit renders the channel infunctonal:

$$F(\text{funct}) = P(wwww)$$

(2) The presence of 2 m subunits renders the channel infunctonal:

$$F(\text{funct}) = P(wwww) + P(wwvm)$$

(3) The presence of 3 m subunits renders the channel infunctonal:

$$F(\text{funct}) = P(wwww) + P(wwvm) + P(wvmm)$$

(4) The presence of 4 m subunits renders the channel infunctonal:

$$F(\text{funct}) = P(wwww) + P(wwvm) + P(wvmm) + P(mmmm)$$

Results and Discussion

Characterization of control and LQT1 induced pluripotent stem cells

When tested for expression of pluripotency markers, all putative induced pluripotent stem cell (iPSC) lines exhibited a strong alkaline phosphatase activity and were immunoreactive for embryonic stem cell-associated antigens, such as the transcription factor NANOG and the surface marker TRA1-81. Moreover, qRT-PCR analysis revealed that all iPSC clones had reactivated endogenous pluripotency genes (*OCT3/4*, *SOX2*, *NANOG*, *REX1*, and *CRIP1/TGFI*), which were expressed at considerably higher levels in reprogrammed pluripotent cells as compared to parental fibroblasts, while transcription levels of the endogenous *KLF4* and *c-MYC* loci were similar (Supplementary Figure 1A). In all established iPSC lines transgenic expression of the 4 reprogramming factors was reduced to low or undetectable levels, comparable to those of the corresponding fibroblasts prior to retroviral infection (Supplementary Figure 1B).

Cardiac differentiation of iPSCs

To direct both iPSC-LQT1 and iPSC-Control into the cardiac lineage, we developed a protocol in which iPSC clones were removed from their feeder layer, grown as floating iPSC spheres for 3 days (Supplementary Figure 3A i), and then induced to differentiate as attached embryoid bodies (EBs) in a defined media (Supplementary Figure 3A ii). Spontaneous beating foci started to appear after 12 days of differentiation in both iPSC-LQT1 and iPSC-Control derived EBs and consisted of cells expressing cardiac specific markers, as cardiac Troponin T (cTNT) (Supplementary Figure 3B). Once micro-dissected and plated onto fibronectin, beating explants were remarkably stable over the time of 3 months and matured further, as assessed by the level of sarcomeric organization for cTNT (Supplementary Figure 3A iii and 3C-D). After collagenase digestion, single dissociated cells from both iPSC-LQT1 and iPSC-Control explants could be re-seeded on fibronectin-coated dishes and cultured up to 2 weeks with maintenance of their beating ability and expression of distinct myocytic markers (Supplementary Figure 3A iv and Figure 2A).

Cardiomyocyte subtype classification of iPSC-Control and iPSC-LQT1 generated cells

At the time window of differentiation that we analyzed in this study (30-90 days), a clear heterogeneity in action potential (AP) morphology was observed, as already reported in the literature for mouse and human ESC- and iPSC-generated cardiomyocytes⁴⁻⁷. However, APs could be classified into 3 major types: “nodal”, “atrial”, and “ventricular” based on distinct AP properties. “Ventricular” APs could be distinguished by the presence of a marked plateau phase resulting in a longer AP duration (APD) and an APD90/APD50 ratio in the range of 1.1 to 1.3. “Atrial” APs presented a more triangular shape with a higher APD90/APD50 ratio between 1.3 and 1.6, a reduced overshoot value, and faster spontaneous rates of activity compared to “ventricular” APs. “Nodal” APs were characterized by less negative maximum diastolic potential (MDP), slower upstroke (dV/dt_{max}) and smaller AP amplitude (APA). Several groups have described the characteristics of APs recorded in spontaneously beating cardiac myocytes derived from human ESCs^{5, 6, 8-10} and human iPSCs⁷. Although slightly different AP values, in particular in APDs, were reported for similar beating frequency, cell maturation and temperature, dependent on the technique used (sharp microelectrodes on clusters of cells or patch-clamp recordings on single isolated cells), the hallmark characteristics of AP sub-types were similar and corresponded to an embryonic phenotype.

AP classification according to these characteristics, illustrated in Fig. 2B of the manuscript and Supplementary Table 2 and 3, was corroborated by gene expression analysis of specific myocytic lineage markers, namely ventricular myosin light chain 2 (MLC2v) for “ventricular” myocytes, atrial myosin light chain (MLC2a) for “atrial” myocytes and the hyperpolarization-activated cyclic nucleotide-gated channel 4 (HCN4) for “nodal” myocytes, as demonstrated by single-cell RT-PCR experiments on patched cells after electrophysiological characterization (Supplementary Figure 4 and 5A). However, single-cell RT-PCR also revealed co-expression of both MLC2a and MLC2v in cells which were characterized by “ventricular” APs and fast spontaneous rate of activity (Supplementary Figure 5B). Co-immunostaining at different stages of myocytic maturation has

confirmed that both MLC2 isoforms were present in approximately 50% of the MLC2v positive cells at 30 days of differentiation and this percentage decreased to approximately 15% after 3 months (Supplementary Figure 5C-E). Although HCN4 mRNA was detectable only in “nodal” cells, “atrial” and “ventricular” myocytes may express other HCN channel isoforms, as already reported for HCN2 in 2-3 months old human ESC-derived and adult cardiomyocytes^{6, 11}, which would account for the I_f diastolic current measured in “ventricular” cells (Supplementary Figure 10).

Fluorescence resonance energy transfer (FRET) measurements and interaction between wild-type KCNQ1 and R190Q-KCNQ1

To assess whether the mutated R190Q-KCNQ1 subunits retain their ability to form multimers with wild-type KCNQ1 subunits, we performed FRET measurements that have already been successfully used to investigate the ability of different types of KCNQ channels to form heteromultimers¹². When wild-type KCNQ1 fused to a cyan fluorescent protein (CFP-WT-KCNQ1) was co-expressed with wild-type KCNQ1 fused to a yellow fluorescent protein (YFP-WT-KCNQ1) in HEK293T cells, both fusion proteins were co-localized in internal membranous structures throughout the cell with exclusion of the nuclei. A robust FRET signal was measured in an acceptor photobleaching assay, suggesting co-assembly of CFP- and YFP-tagged wild-type KCNQ1 subunits (Supplementary Figure 9A and 9D). Co-expression of CFP-WT-KCNQ1 and YFP-R190Q-KCNQ1 yielded a virtually identical FRET efficiency, indicating that the ability of the KCNQ1 subunits to form tetramers is not affected by the R190Q mutation (Supplementary Figure 9B and 9D). To exclude that this FRET signal is caused by a high local concentration of the fusion proteins in the internal membranes rather than by proximity of the fluorochromes due to a direct specific interaction of the ion channel subunits, we performed control experiments on cells co-transfected with CFP-WT-KCNQ1 and a fusion protein of YFP and the β -adrenergic receptor 1 (YFP- β_1 -R). When imaged at 6-8 hours after transfection, YFP- β_1 -R co-localized with CFP-WT-KCNQ1 in internal membranous structures while only a faint staining of the plasma membrane was seen in

some cells. However, no significant FRET signal was measured (Supplementary Figure 9C and 9D), even though the expression level of YFP- β_1 -R was comparable to that of the YFP-fused KCNQ1 subunits. We conclude that the FRET measured between CFP-WT-KCNQ1 and YFP-R190Q-KCNQ1 indeed represents a specific interaction between the channel subunits.

2. Supplementary Tables

Supplementary Table 1. Primers used for sequencing of the human *KCNQ1* gene (exon 2), for RT-PCR, qRT-PCR, and TaqMan assay for allelic discrimination.

Gene	Use	Primer forward	Primer reverse
<i>KCNQ1-ex2</i>	Sequencing	AGGGTCTGAAGCCACTCAA	TAAACGGAGAGACCCAACT
<i>c-MYC</i> endogenous	qRT-PCR	AGAAATGTCCTGAGCAATCACC	AAGGTTGTGAGGTTGCATTTGA
<i>KLF4</i> endogenous	qRT-PCR	ATAGCCTAAATGATGGTGCTTGG	AACCTTTGGCTTCCTTGTITGG
<i>OCT3/4</i> endogenous	qRT-PCR	GACAGGGGGAGGGGAGGAGCTAGG ¹⁵	CTTCCCTCCAACCAGTTGCCCAAAC ¹⁵
<i>SOX2</i> endogenous	qRT-PCR	GGGAAATGGGAGGGGTGCAAAGAGG ¹⁵	TTGCGTGAGTGTGGATGGGATTGGTG ¹⁵
<i>NANOG</i>	qRT-PCR	TGCAAGAACTCTCCAACATCCT	ATTGCTATTCTTCGGCCAGTT
<i>REX1</i>	qRT-PCR	ACCAGCACACTAGGCAAACC	TTCTGTTACACAGGCTCCA
<i>TDGF1</i>	qRT-PCR	CCCAAGAAGTGTTCCCTGTG	ACGTGCAGACGGTGGTAGTT
<i>MYC</i> transgene	qRT-PCR	GGAAACGACGAGAACAGTTGA	CCCTTTTTCTGGAGACTAAATAAA ¹⁵
<i>KLF4</i> transgene	qRT-PCR	CCACCTCGCCTTACACATGA	CCCTTTTTCTGGAGACTAAATAAA ¹⁵
<i>OCT3/4</i> transgene	qRT-PCR	GCTCTCCCATGCATTCAAAC	TTATCGTCGACCACTGTGCTGCTG ¹⁵
<i>SOX2</i> transgene	qRT-PCR	GGCCATTAACGGCACACTG	CCCTTTTTCTGGAGACTAAATAAA ¹⁵
<i>PDX1</i>	qRT-PCR	AAGCTCACGCGTGGAAG	GGCCGTGAGATGTACTTGTG
<i>SOX7</i>	qRT-PCR	TGAACGCCTTCATGGTTTG	AGCGCCTTCCACGACTTT
<i>AFP</i>	qRT-PCR	GTGCCAAGCTCAGGGTGTAG	CAGCCTCAAGTTGTTCTCTCTG
<i>CD31</i>	qRT-PCR	ATGCCGTGGAAAGCAGATAC	CTGTTCTTCTCGGAACATGGA
<i>DES</i>	qRT-PCR	GTGAAGATGGCCCTGGATGT	TGGTTTCTCGGAAGTTGAGG
<i>ACTA2</i>	qRT-PCR	GTGATCACCATCGGAAATGAA	TCATGATGCTGTTGTAGGTGGT
<i>SCL</i>	qRT-PCR	CCAACAATCGAGTGAAGAGGA	CCGGCTGTTGGTGAAGATAC
<i>MYL2</i>	qRT-PCR	TACGTTTCGGGAAATGCTGAC	TTCTCCGTGGGTGATGATG
<i>CDH5</i>	qRT-PCR	GAGCATCCAGGCAGTGGTAG	CAGGAAGATGAGCAGGGTGA
<i>KRT14</i>	qRT-PCR	CACCTCTCCTCCTCCAGTT	ATGACCTTGGTGCGGATTT
<i>NCAM1</i>	qRT-PCR	CAGATGGGAGAGGATGGAAA	CAGACGGGAGCCTGATCTCT
<i>TH</i>	qRT-PCR	TGTAAGGTTTACGGTGGAGT	TCTCAGGCTCCTCAGACAGG
<i>GABRR2</i>	qRT-PCR	CTGTGCCTGCCAGAGTTTCA	ACGGCCTTGACGTAGGAGA
<i>KCNQ1</i>	qRT-PCR	CGCCTGAACCGAGTAGAAGA	TGAAGCATGTCGGTGATGAG
<i>cTNT</i>	qRT-PCR	AGCATCTATAACTTGGAGGCAGAG	TGGAGACTTTCTGGTTATCGTTG
<i>GAPDH</i>	qRT-PCR/RT-PCR	TCCTCTGACTTCAACAGCGA	GGGTCTTACTCCTTGGAGGC
<i>MYL7 (MLC2a)</i>	RT-PCR	CCGTCTTCTCACGCTCTT	TGAACTCATCCTTGTTCACCAC
<i>HCN4</i>	RT-PCR	CAATGAGGTGCTGGAGGAGT	GGTCGTGCTGGACTTTGTG
<i>MYL2 (MLC2v)</i>	RT-PCR	TACGTTTCGGGAAATGCTGAC	TTCTCCGTGGGTGATGATG
<i>KCNQ1-569G to KCNQ1-569A</i>	allelic discrimination	Custom TaqMan SNP Genotyping assays, Small-Scale, Human. Assay ID: AHVINMR	

Supplementary Table 2. Action potential properties of spontaneously beating cardiomyocytes derived from control and LQT1 induced pluripotent stem cell (iPSC) lines

	Cell n°	Beating rate (bpm)	Overshoot (mV)	MDP (mV)	Upstroke velocity (dV/dt _{max})	APD50 (msec)	APD90 (msec)	APD (msec)	V _{Rep} (V/sec)	APA (mV)
iPSC-Control derived cardiomyocytes										
Ventricular	21	68.2 ± 2.7	44.0 ± 1.5	-63.5 ± 2.1	9.0 ± 0.2	323.3 ± 30.3	381.3 ± 35.3	433.7 ± 39.1	0.28 ± 0.02	107.8 ± 2.1
Atrial	7	95.6 ± 9.9	25.0 ± 2.5	-63.8 ± 2.2	8.6 ± 0.8	73.7 ± 11.6	104.4 ± 13.1	141.8 ± 15.5	0.66 ± 0.06	88.7 ± 3.1
Nodal	6	66.9 ± 4.3	27.1 ± 2.7	-44.1 ± 3.6	4.3 ± 0.3	139.1 ± 12.2	206.6 ± 8.3	269.7 ± 4.5	0.26 ± 0.01	71.3 ± 4.1
iPSC-LQT1 derived cardiomyocytes										
Ventricular	14	59.9 ± 2.2	45.5 ± 2.1	-64.9 ± 2.6	8.4 ± 0.2	654.0 ± 87.7*	745.2 ± 91.4*	804.7 ± 93.4*	0.16 ± 0.01*	110.4 ± 2.8
Atrial	10	99.3 ± 4.7	24.6 ± 2.7	-63.7 ± 2.4	8.9 ± 0.9	171.6 ± 15.9*	221.4 ± 20.0*	267.4 ± 23.0*	0.40 ± 0.03*	88.2 ± 3.0
Nodal	5	62.5 ± 1.0	29.9 ± 1.8	-45.4 ± 3.0	4.5 ± 0.4	122.8 ± 28.3	197.0 ± 25.3	268.7 ± 24.8	0.29 ± 0.02	75.2 ± 3.5

Values are mean ± SE. **P*<0.05 LQT1 vs control group (one-way ANOVA). MDP, maximum diastolic potential; APD50/APD90, AP duration measured at 50% or 90% repolarization; APD, AP duration; V_{rep}, repolarization velocity; APA, AP amplitude.

Supplementary Table 3. Action potential properties of cardiac myocytes derived from control and LQT1 induced pluripotent stem cell (iPSC) lines paced at 1Hz

	Cell n°	Overshoot (mV)	MDP (mV)	APD50 (msec)	APD90 (msec)	APD (msec)	V _{rep} (V/sec)	APA (mV)
iPSC-Control derived cardiomyocytes								
Ventricular	40	42.4 ± 0.7	-65.5 ± 1.2	317.5 ± 19.4	373.2 ± 22.6	426.0 ± 25.3	0.30 ± 0.01	108.0 ± 1.2
Atrial	14	27.9 ± 3.1	-64.5 ± 2.7	85.4 ± 13.8	119.9 ± 15.5	162.3 ± 18.1	0.59 ± 0.06	92.4 ± 1.7
Nodal	10	25.1 ± 1.8	-46.0 ± 2.5	127.3 ± 16.7	191.1 ± 23.2	251.7 ± 29.7	0.36 ± 0.08	71.1 ± 2.5
iPSC-LQT1 derived cardiomyocytes								
Ventricular	36	43.8 ± 0.8	-66.6 ± 1.2	480.8 ± 33.8**	554.2 ± 35.6**	606.0 ± 36.8**	0.20 ± 0.01**	110.3 ± 1.3
Atrial	16	34.6 ± 1.6	-63.3 ± 1.8	137.3 ± 20.7*	190.8 ± 28.1*	244.3 ± 32.0*	0.43 ± 0.05	97.9 ± 2.9
Nodal	4	29.1 ± 0.4	-51.3 ± 6.0	129.4 ± 4.9	199.5 ± 9.1	278.0 ± 8.7	0.29 ± 0.03	80.3 ± 6

Values are mean ± SE. **P*<0.05, ***P*<0.001 LQT1 vs control group (one-way ANOVA). MDP, maximum diastolic potential; APD50/APD90, AP duration measured at 50% or 90% repolarization; APD, AP duration; V_{rep}, repolarization velocity; APA, AP amplitude.

3. Supplementary Figures

Supplementary Figure 1. Re-expression of endogenous genes associated with pluripotency and silencing of the transgenes in induced pluripotent stem cell (iPSC) clones from control and LQT1 individuals.

Supplementary Figure 2. Up-regulation of lineage markers representative of the three embryonic germ layers in induced pluripotent stem cell (iPSC) clones from control and LQT1 individuals.

Supplementary Figure 3. *In vitro* cardiac differentiation of control and LQT1 induced pluripotent stem cells (iPSCs).

Supplementary Figure 4. Molecular markers and action potential parameters used for the classification of “ventricular”, “atrial”, and “nodal” cardiomyocytes derived from induced pluripotent stem cells (iPSCs).

Supplementary Figure 5. Expression of MLC2a, MLC2v, and HCN4 in myocytes derived from induced pluripotent stem cells (iPSCs).

Supplementary Figure 6. Action potential rate adaptation in “ventricular” myocytes derived from control and LQT1 induced pluripotent stem cells.

Supplementary Figure 7. Action potential parameters of “ventricular” myocytes obtained from different induced pluripotent stem cell (iPSC) clones at stimulation rate of 1Hz.

Supplementary Figure 8. *KCNQ1* mRNA and protein levels in myocytes from control and LQT1 induced pluripotent stem cells and allelic expression of wild-type and mutated 569G>A transcripts in LQT1 cells.

Supplementary Figure 9. Fluorescence Resonance Energy Transfer (FRET) analysis of interaction between wild-type *KCNQ1* and R190Q-*KCNQ1*.

Supplementary Figure 10. I_{to} and diastolic currents of “ventricular” myocytes from control and LQT1 induced pluripotent stem cells (iPSCs).

4. Supplementary Movie Legends

Supplementary Movie 1. Beating foci in an embryoid body from LQT1 induced pluripotent stem cells at day 12 of differentiation (Patient II-2, clone a).

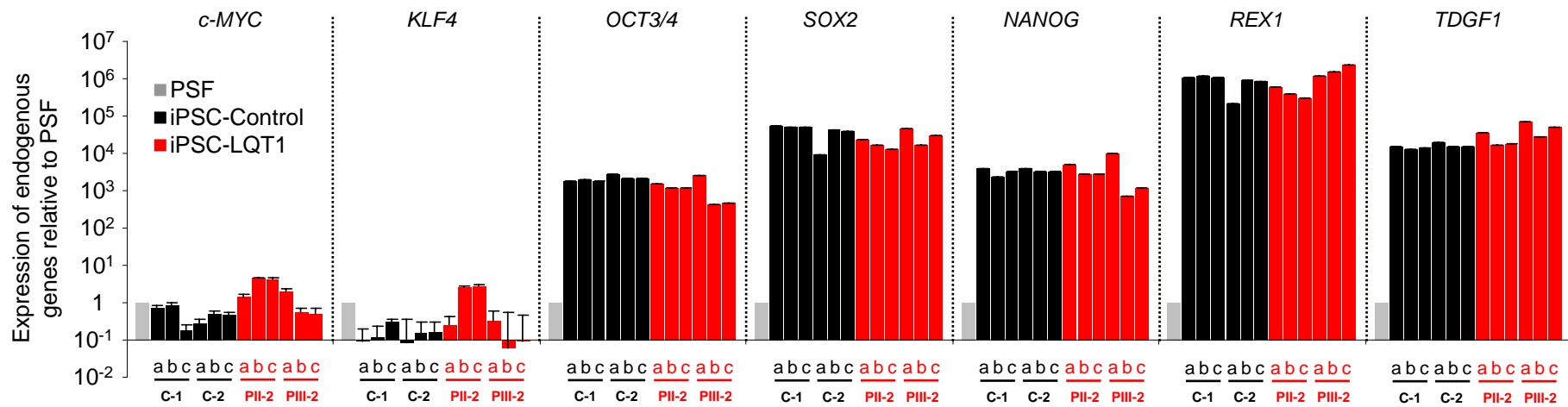
Supplementary Movie 2. Beating single myocytes dissociated from a LQT1 explant (Patient III-2, clone c).

5. Supplementary References

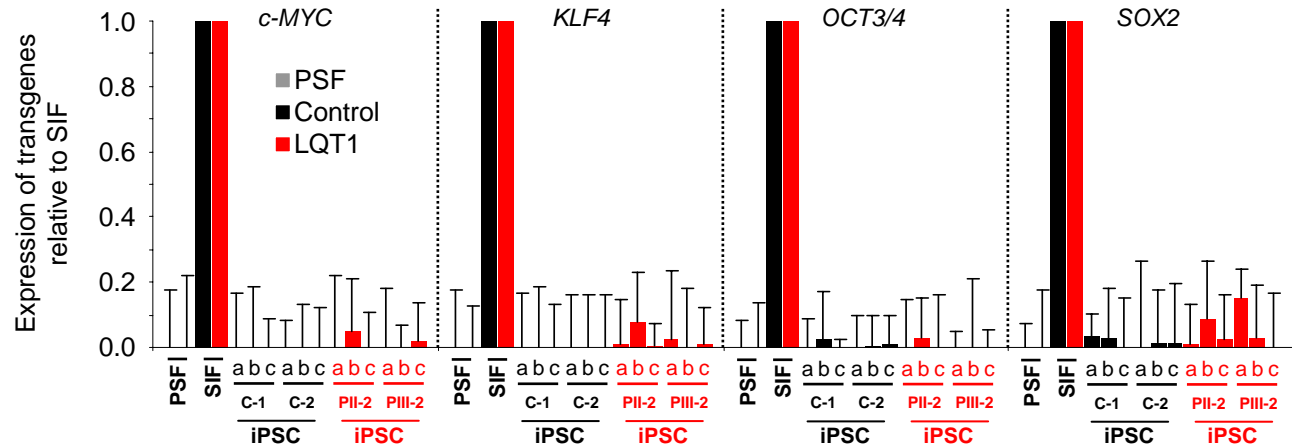
1. Chen X, Weaver J, Bove BA, et al. Allelic imbalance in BRCA1 and BRCA2 gene expression is associated with an increased breast cancer risk. *Hum Mol Genet* 2008;17:1336-48.
2. Hamill OP, Marty A, Neher E, Sakmann B, Sigworth FJ. Improved patch-clamp techniques for high-resolution current recording from cells and cell-free membrane patches. *Pflugers Arch* 1981;391:85-100.
3. Voigt P, Dorner MB, Schaefer M. Characterization of p87PIKAP, a novel regulatory subunit of phosphoinositide 3-kinase gamma that is highly expressed in heart and interacts with PDE3B. *J Biol Chem* 2006;281:9977-86.
4. David R, Stieber J, Fischer E, et al. Forward programming of pluripotent stem cells towards distinct cardiovascular cell types. *Cardiovasc Res* 2009;84:263-72.
5. He JQ, Ma Y, Lee Y, Thomson JA, Kamp TJ. Human embryonic stem cells develop into multiple types of cardiac myocytes: action potential characterization. *Circ Res* 2003;93:32-9.
6. Sartiani L, Bettiol E, Stillitano F, Mugelli A, Cerbai E, Jaconi ME. Developmental changes in cardiomyocytes differentiated from human embryonic stem cells: a molecular and electrophysiological approach. *Stem Cells* 2007;25:1136-44.
7. Zhang J, Wilson GF, Soerens AG, et al. Functional cardiomyocytes derived from human induced pluripotent stem cells. *Circ Res* 2009;104:e30-41.
8. Mummery C, Ward-van Oostwaard D, Doevendans P, et al. Differentiation of human embryonic stem cells to cardiomyocytes: role of coculture with visceral endoderm-like cells. *Circulation* 2003;107:2733-40.
9. Jonsson MK, Duker G, Tropp C, et al. Quantified proarrhythmic potential of selected human embryonic stem cell-derived cardiomyocytes. *Stem Cell Res. Epub* 2010 Feb17.
10. Peng S, Lacerda AE, Kirsch GE, Brown AM, Bruening-Wright A. The action potential and comparative pharmacology of stem cell-derived human cardiomyocytes. *J Pharmacol Toxicol Methods. Epub* 2010 Feb11.
11. Baruscotti M, Barbuti A, Bucchi A. The cardiac pacemaker current. *J Mol Cell Cardiol* 2010;48:55-64.
12. Bal M, Zhang J, Zaika O, Hernandez CC, Shapiro MS. Homomeric and heteromeric assembly of KCNQ (Kv7) K⁺ channels assayed by total internal reflection fluorescence/fluorescence resonance energy transfer and patch clamp analysis. *J Biol Chem* 2008;283:30668-76.

Supplementary Figure 1

A



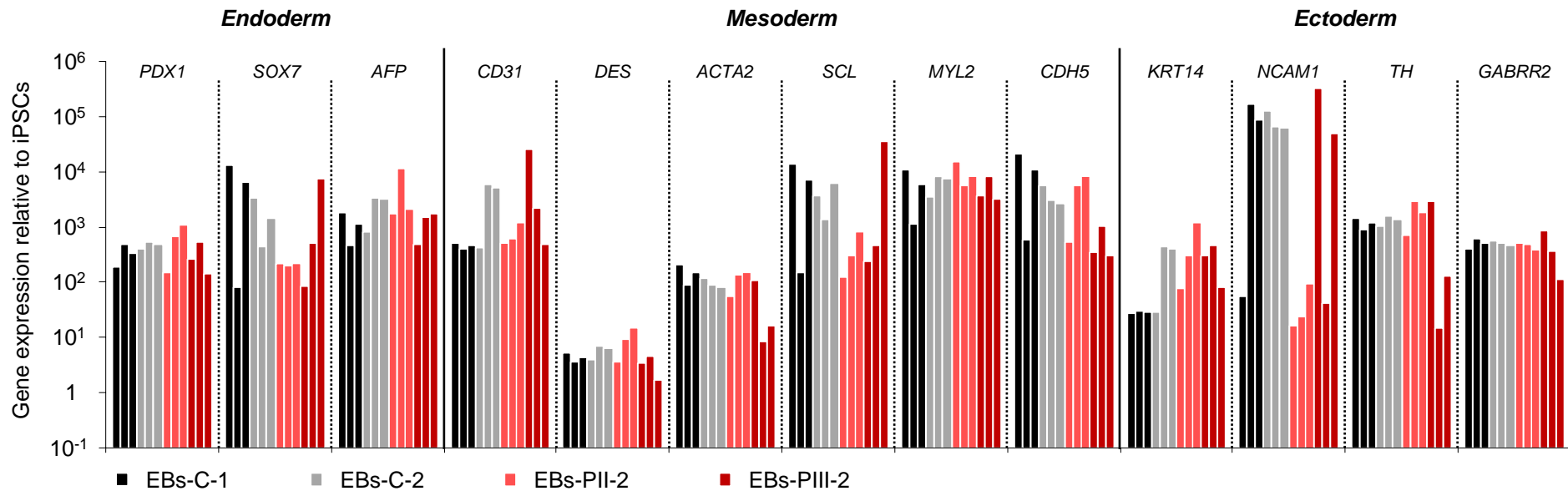
B



Supplementary Figure 1. Re-expression of endogenous genes associated with pluripotency and silencing of the transgenes in induced pluripotent stem cell (iPSC) clones from control and LQT1 individuals.

Panel A shows qRT-PCR analysis of the endogenous pluripotency associated genes (*c-MYC*, *KLF4*, *OCT3/4*, *SOX2*, *NANOG*, *REX1*, and *TDGF1*) revealing similar activation of these genes in all three iPSC clones (a, b, and c) derived from each control individual (C-1 and C-2, black bars) and LQT1 patient (PII-2 and PIII-2, red bars). Expression values are relative to corresponding primary skin fibroblasts (PSF, grey bars). Panel B shows qRT-PCR analysis of the four transgenes used for the reprogramming, *c-MYC*, *KLF4*, *OCT3/4*, and *SOX2*, in all three iPSC clones (a, b, and c) derived from each control individual (C-1 and C-2, black bars) and LQT1 patient (PII-2 and PIII-2, red bars). Transgenes silencing is demonstrated by expression levels similar to parental PSF (C-1 and PII-2). Expression values are relative to skin fibroblasts after the retroviral infection (SIF, C-1 and PII-2). Expression values in panels A and B are normalized to *GAPDH* and are presented as mean \pm SE, $n=3$.

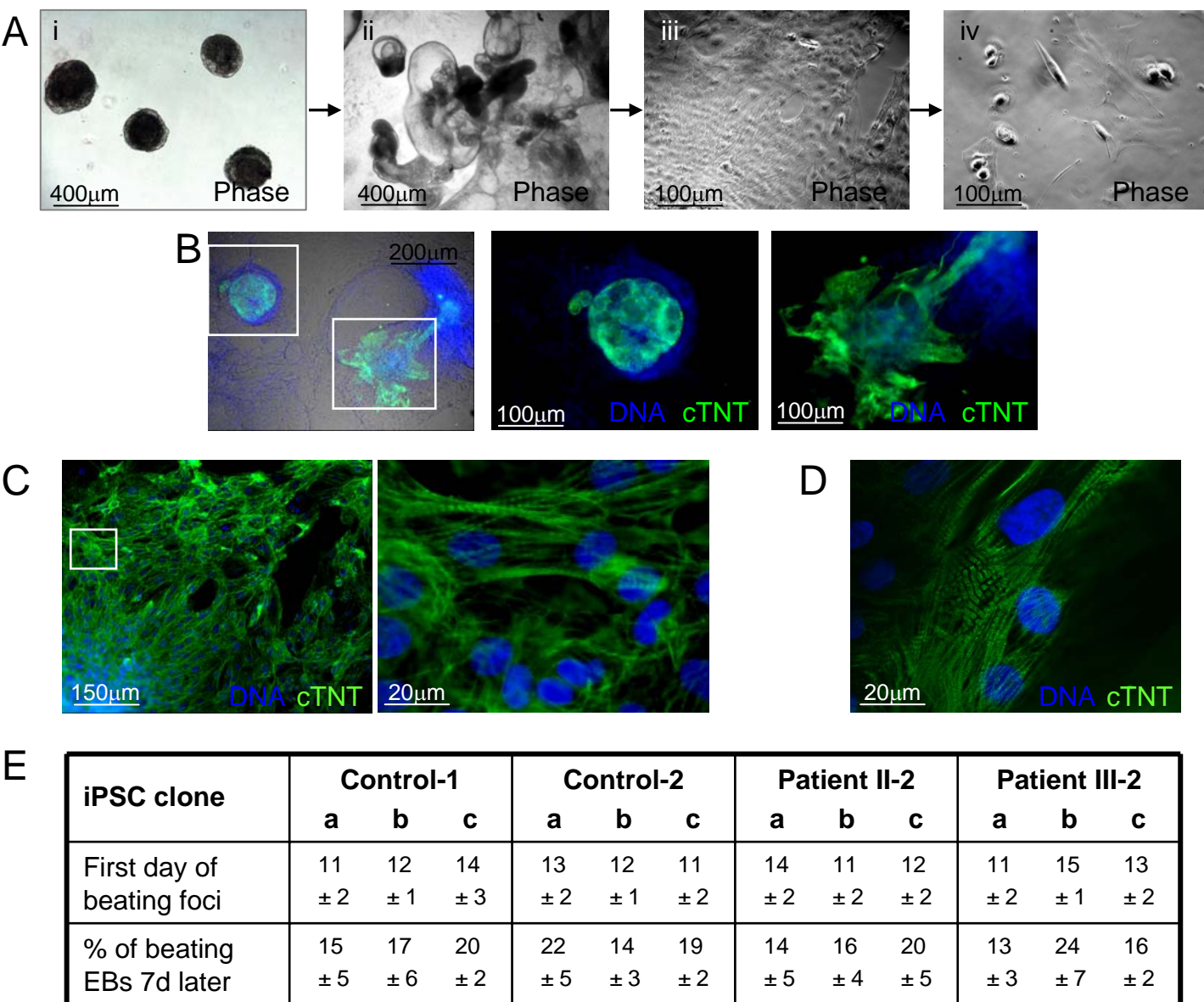
Supplementary Figure 2



Supplementary Figure 2. Up-regulation of lineage markers representative of the three embryonic germ layers in induced pluripotent stem cell (iPSC) clones from control and LQT1 individuals.

The bar graph shows qRT-PCR analysis of markers of the three different germ layers, endoderm (*PDX1*, *SOX7*, and *AFP*), mesoderm (*CD31*, *DES*, *ACTA2*, *SCL*, *MYL2*, and *CDH5*), and ectoderm (*KRT14*, *NCAM1*, *TH*, and *GABRR2*) in embryoid bodies (EBs) at day 21 of differentiation from three iPSC clones (a, b, and c) derived from each control individual (C-1, black bars and C-2, grey bars) and LQT1 patient (P1I-2, light red bars and P1II-2, dark red bars). Gene expression values are relative to corresponding undifferentiated iPSC clones, normalized to *GAPDH*, and presented as mean \pm SE, n=3.

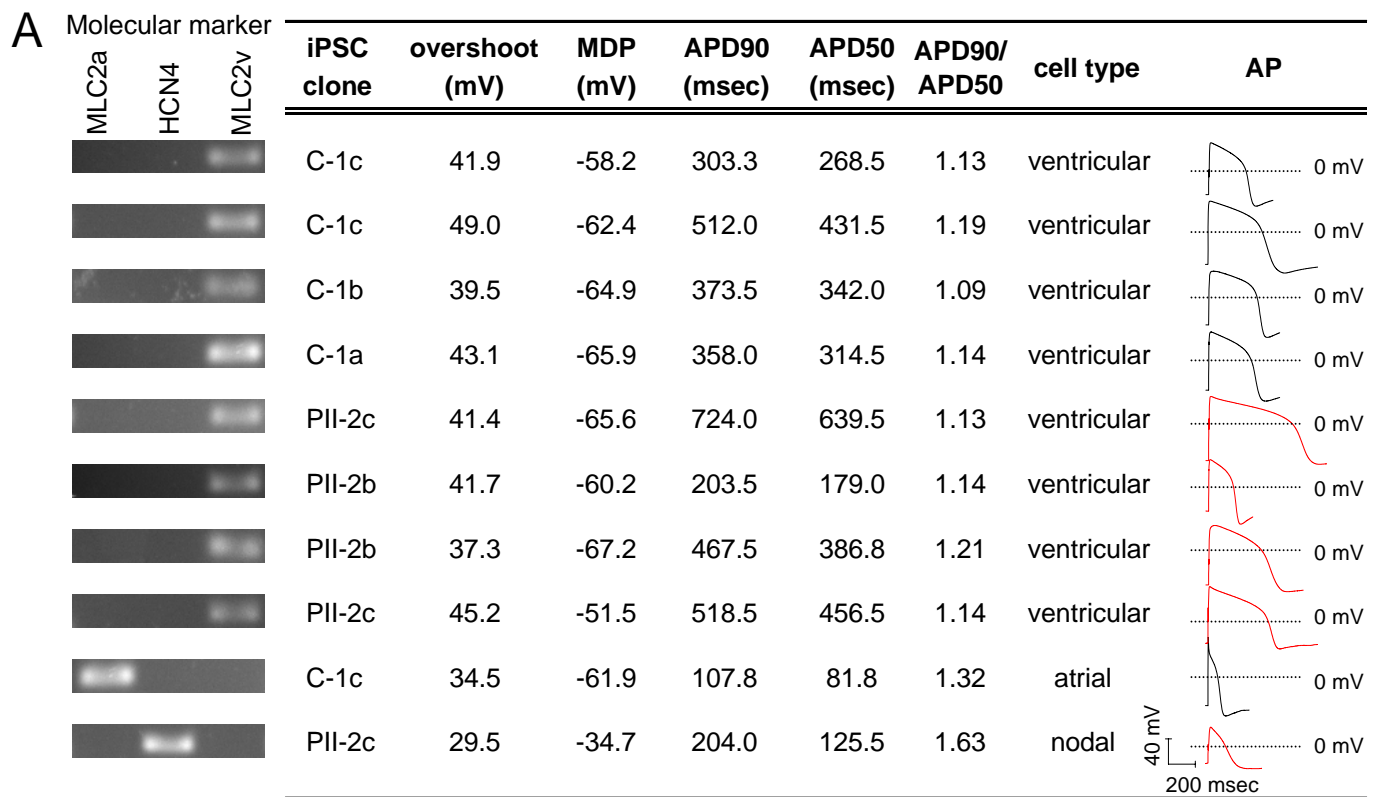
Supplementary Figure 3



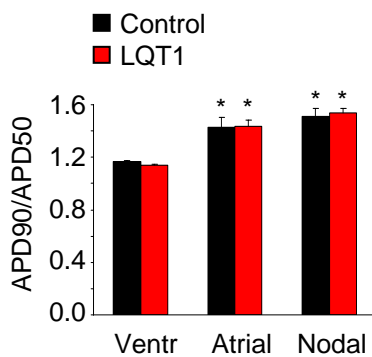
Supplementary Figure 3. *In vitro* cardiac differentiation of control and LQT1 induced pluripotent stem cells (iPSCs).

Panel A is a representation of the *in vitro* differentiation process into the cardiac lineage. iPSC colonies were differentiated as floating embryoid bodies (EBs) (i) and then plated down on gelatin (ii) to detect beating foci. Beating areas were micro-dissected and plated on fibronectin (iii). These explants were dissociated into single cells (iv) for immunohistochemical and electrophysiological analyses. Panel B shows immunofluorescence detection of cardiac Troponin T (cTNT) protein in attached EBs from a representative iPSC-LQT1 clone (Patient II-2, clone c); middle and right panels represent magnifications of the areas framed in the left panel. Panel C shows immunofluorescence detection of cTNT in a representative explant from iPSC-LQT1 (Patient II-2, clone a), revealing that most of the cells are cardiomyocytes; the right panel represents magnification of the area framed in the left panel. Panel D shows immunofluorescence detection of cTNT in a representative explant from iPSC-Control (Control-1, clone a). Panel E compares cardiac differentiation properties of different iPSC-Control and iPSC-LQT1 clones. Values are the mean \pm SE from four independent experiments.

Supplementary Figure 4



B



	APD90/APD50	
	average ±SE	range
Control		
Ventricular	1.17 ± 0.01	1.07 - 1.30
Atrial	1.43 ± 0.07*	1.32 - 1.62
Nodal	1.51 ± 0.06*	1.34 - 1.94
LQT1		
Ventricular	1.14 ± 0.05	1.06 - 1.30
Atrial	1.44 ± 0.04*	1.35 - 1.54
Nodal	1.54 ± 0.03*	1.46 - 1.63

C

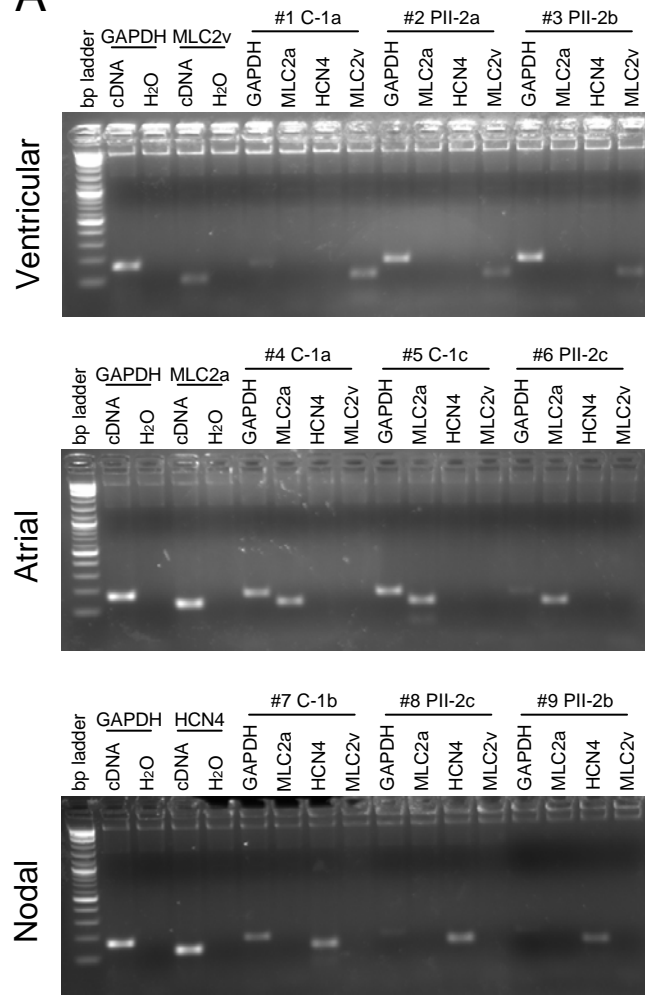
	n	Overshoot (mV)	MDP (mV)
Control			
Ventricular	40	42.4 ± 0.7	-65.5 ± 1.2
Atrial	14	27.9 ± 0.95*	-64.5 ± 2.7*
Nodal	10	25.1 ± 1.8*	-46.0 ± 2.5*
LQT1			
Ventricular	36	43.8 ± 0.8	-66.6 ± 1.2
Atrial	16	34.6 ± 1.6*	-63.3 ± 1.8*
Nodal	4	29.1 ± 0.4*	-51.3 ± 6.0*

Supplementary Figure 4. Molecular markers and action potential parameters used for the classification of “ventricular”, “atrial”, and “nodal” cardiomyocytes derived from induced pluripotent stem cells (iPSCs).

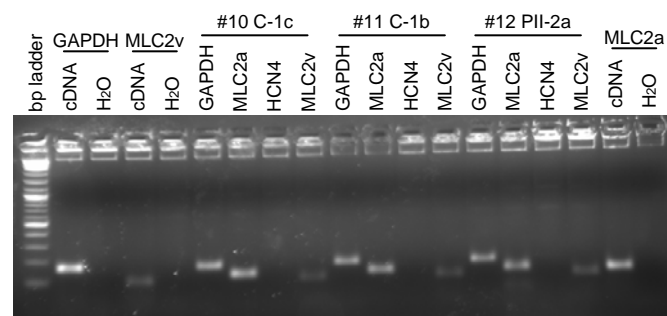
Panel A shows single-cell RT-PCR results for expression of cardiomyocyte specific molecular markers, *MLC2a* (atrial), *HCN4* (nodal), and *MLC2v* (ventricular), in iPSC-derived myocytes after recording their action potential (AP). The table shows iPSC clone, overshoot, MDP, APD90 and APD50 (recorded at stimulation rate of 1Hz), APD90/APD50 ratio, cell type classification, and corresponding AP trace. Panel B shows the APD90/APD50 ratios for “ventricular”, “atrial”, and “nodal” cardiomyocytes in control (black bars) and LQT1 (red bars). Between 4 and 40 cells from six different iPSC clones were analyzed per each group, at 1Hz stimulation rate. This ratio did not differ with change of stimulation frequency or between spontaneous and paced APs. * $P < 0.05$ vs ventricular myocytes (one-way ANOVA on rank, pair-wise multiple comparison procedures using Dunn’s methods). The table shows the average APD90/APD50 ratio obtained for each control and LQT1 iPSC-derived cardiomyocyte subtype and the corresponding range. For “ventricular” and “atrial” cells the ratio range was used as cut-off for cardiomyocyte subtype classification. Panel C shows other AP parameters that differ among cardiomyocytes subtypes and were used for AP classification. * $P < 0.05$ vs ventricular, * $aP < 0.05$ vs ventricular and atrial (one-way ANOVA on rank, pair-wise multiple comparison procedures using Dunn’s methods).

Supplementary Figure 5

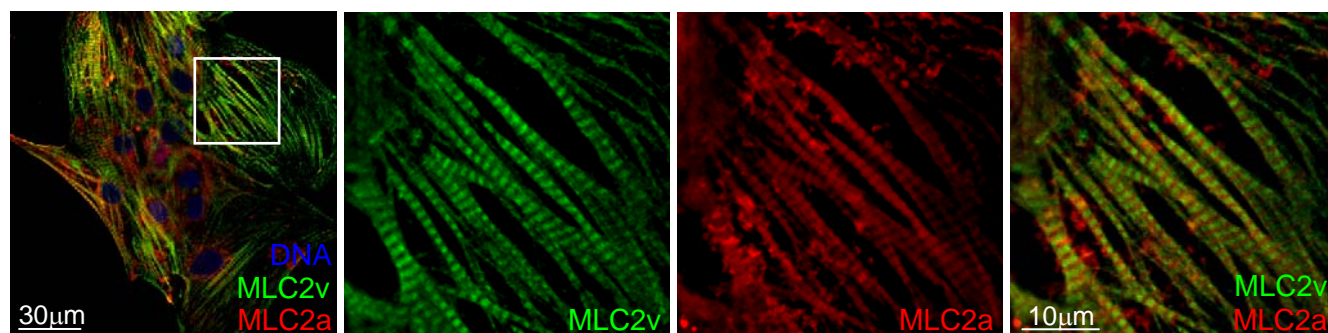
A



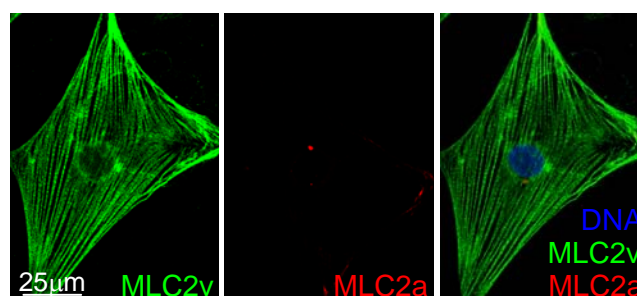
B



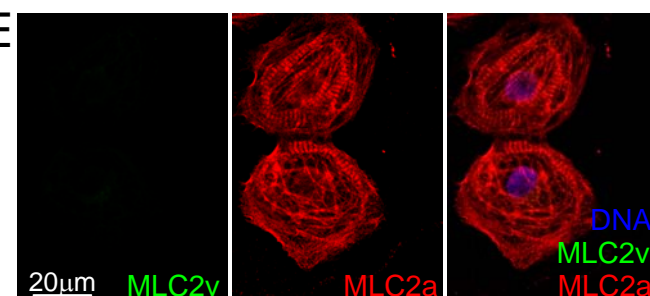
C



D



E

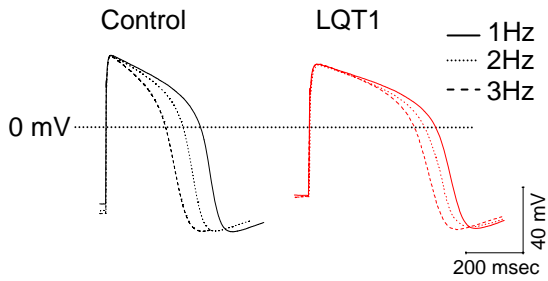


Supplementary Figure 5. Expression of *MLC2a*, *MLC2v*, and *HCN4* in myocytes derived from induced pluripotent stem cells (iPSCs).

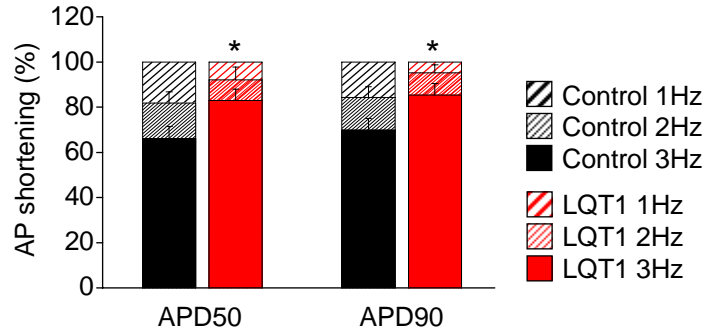
Panel A shows single-cell RT-PCR results for expression of cardiomyocyte specific molecular markers, *MLC2v* (ventricular), *MLC2a* (atrial), and *HCN4* (nodal) in iPSC-derived myocytes from Control-1 and LQT1 Patient II-2 (cell #1 to #9, clones a, b and c). Three different cells per each cardiomyocytic subtype are shown. Panel B shows single-cell RT-PCR results for expression of the same myocytic markers in three cells (#10 to #12) that were positive for both *MLC2a* and *MLC2v*. *GAPDH* was used as loading control. Pooled cDNA from whole embryoid bodies at day 21 was used as positive control. Panels C-E show co-immunofluorescence analysis for *MLC2v* (green) and *MLC2a* (red) in dissociated myocytes from LQT1 explants. Double positive cells for *MLC2v* and *MLC2a* (C) and single positive cells for *MLC2v* (D) or *MLC2a* (E) were found. Magnifications in C refer to the framed area in the left panel.

Supplementary Figure 6

A



B

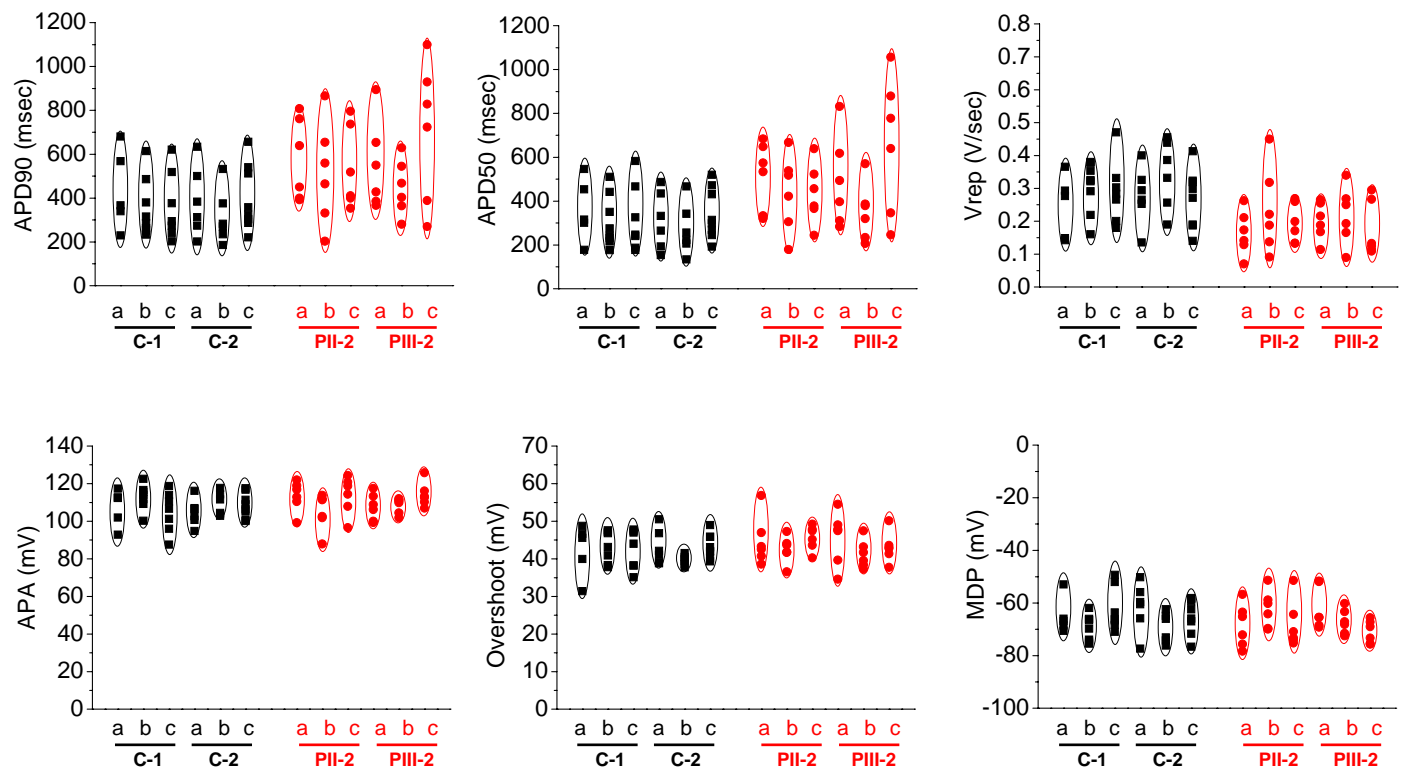


Supplementary Figure 6. Action potential rate adaptation in “ventricular” myocytes derived from control and LQT1 induced pluripotent stem cells.

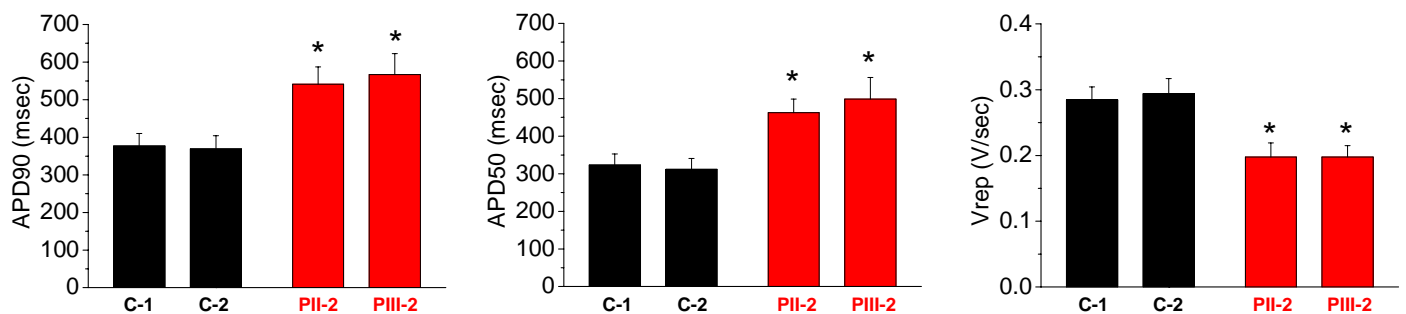
Panel A illustrates overlay of single action potentials from a representative control (black traces) and LQT1 (red traces) cardiomyocyte at 1, 2, and 3Hz stimulation rates. Panel B shows the percentage of APD50 and APD90 shortening during 2 and 3Hz stimulation relative to 1Hz. Data are presented as mean \pm SE, $n=9$ cells in each group (from three Control-1 and three LQT1 Patient II-2 clones). * $P<0.05$ LQT1 vs control myocytes, at 2 and 3Hz (one-way ANOVA).

Supplementary Figure 7

A



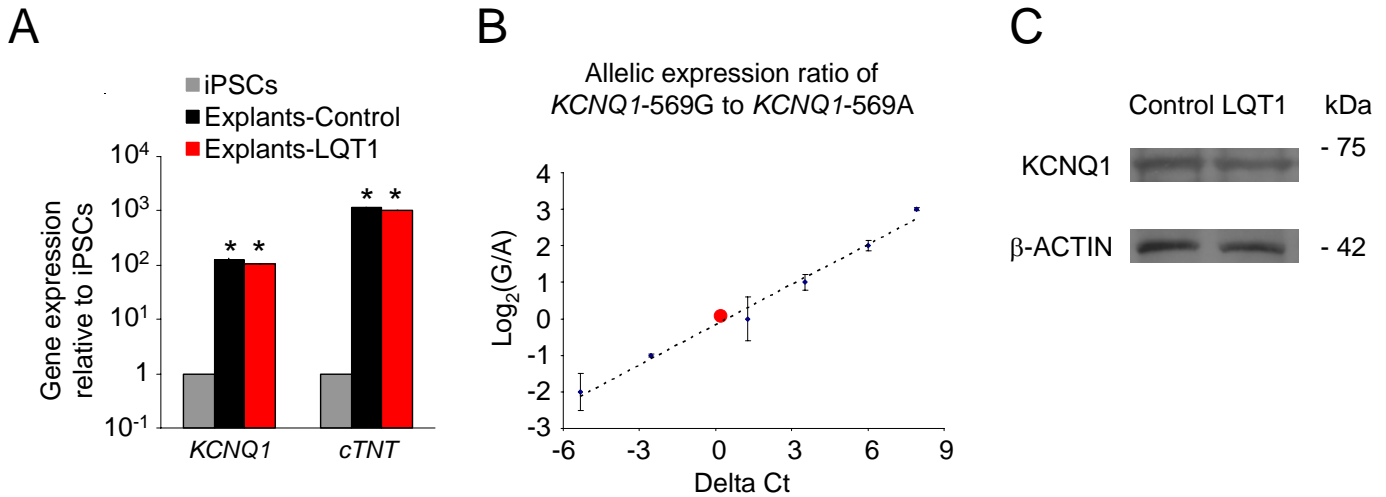
B



Supplementary Figure 7. Action potential parameters of “ventricular” myocytes obtained from different induced pluripotent stem cell (iPSC) clones at stimulation rate of 1Hz.

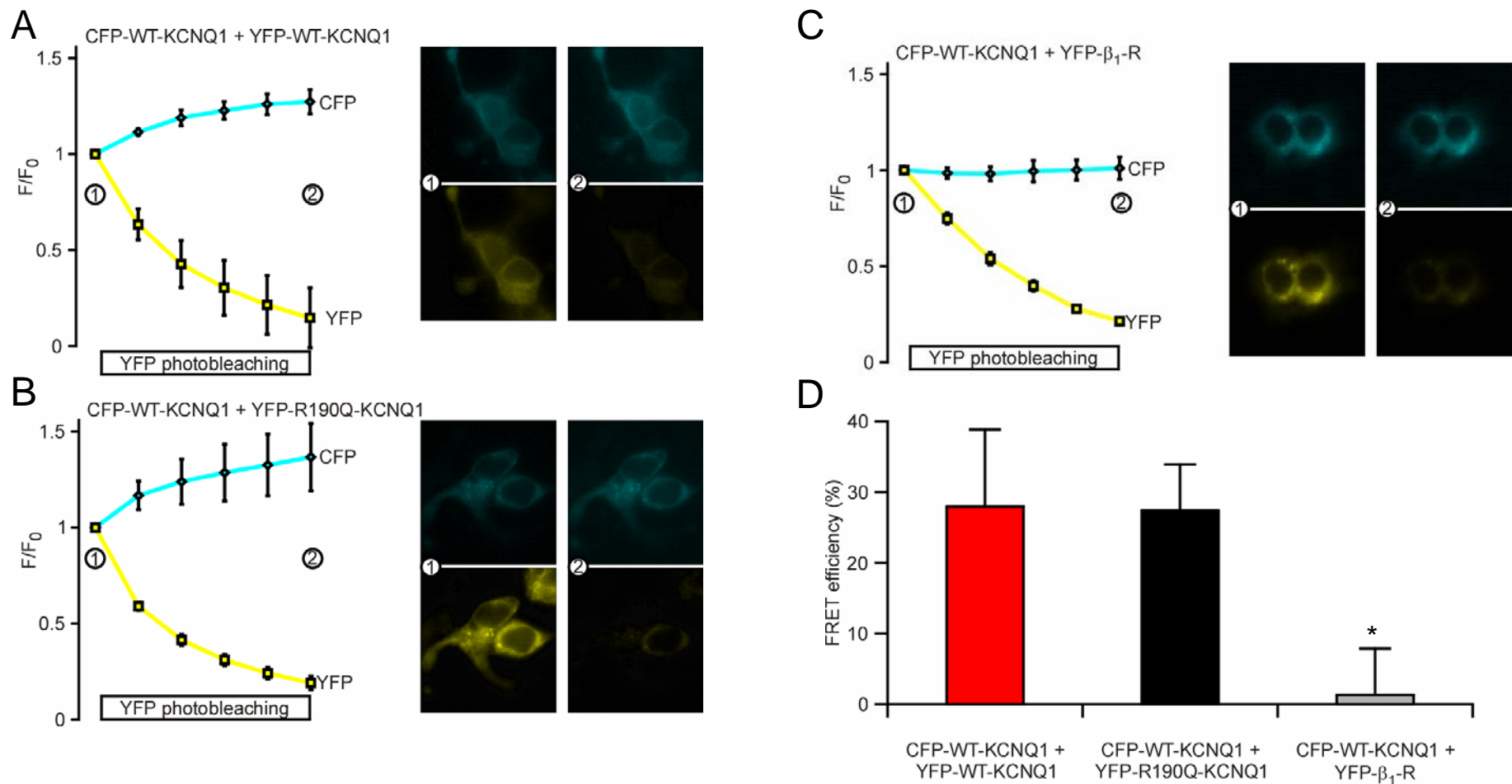
In panel A, three iPSC clones (a, b, and c) derived from each control individual (C-1 and C-2, black) and LQ1 patient (PII-2 and PIII-2, red) are compared. There are no significant differences among clones within control or LQ1 groups using one-way ANOVA or Kruskal-Wallis one-way ANOVA on ranks. In panel B, means \pm SE from each individual are compared using one-way ANOVA or Kruskal-Wallis one-way ANOVA on ranks. Significant differences ($P < 0.05$) between LQ1 and each control group are marked by *.

Supplementary Figure 8



Supplementary Figure 8. *KCNQ1* mRNA and protein levels in myocytes from control and LQT1 induced pluripotent stem cells and allelic expression of wild-type and mutated 569G→A transcripts in LQT1 cells.

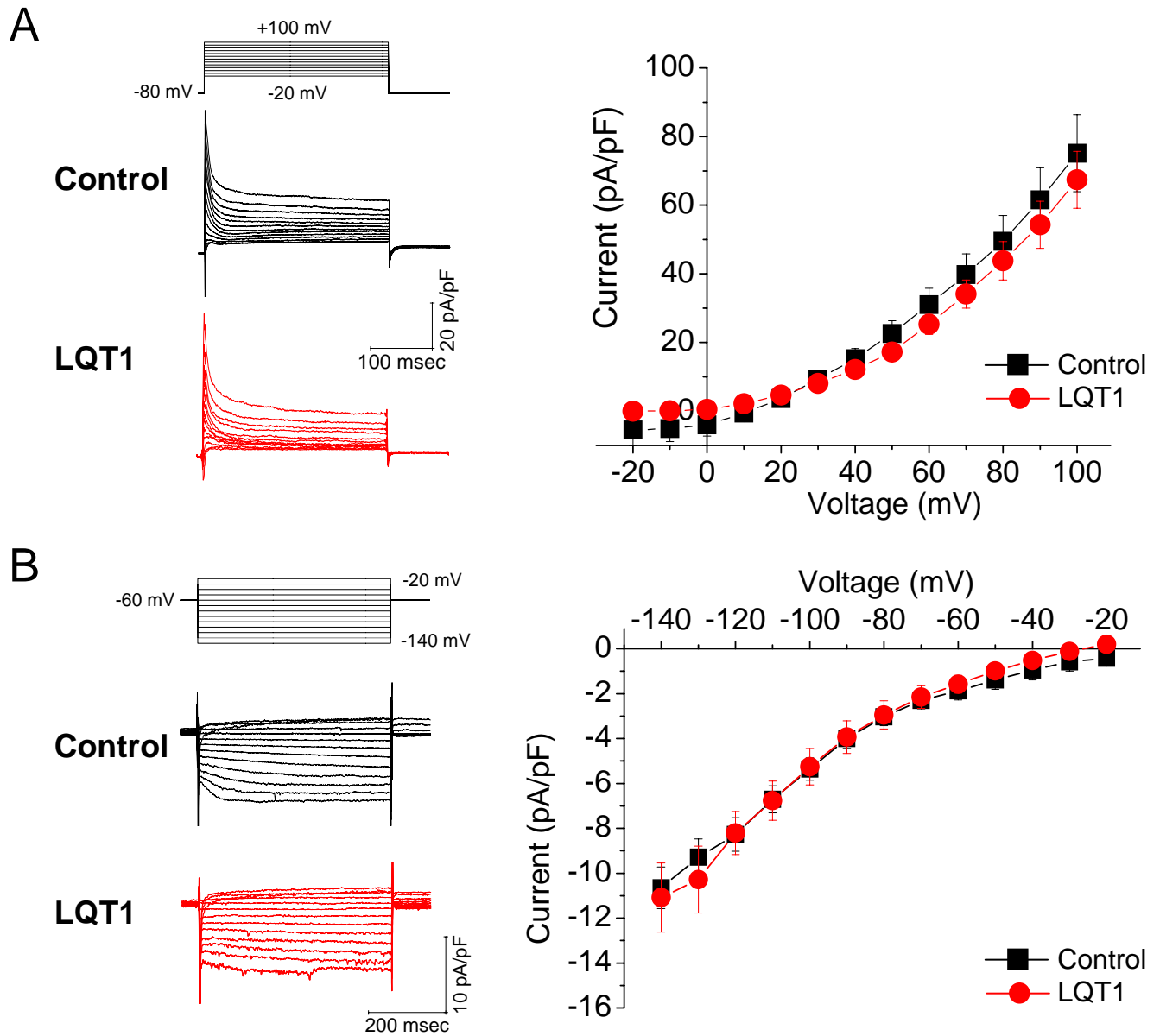
Panel A shows qRT-PCR analysis of *KCNQ1* and *cTNT* revealing similar expression levels in pooled control (black bars) and LQT1 (red bars) myocytic explants. Expression values are relative to corresponding undifferentiated induced pluripotent stem cells (iPSCs, grey bars), normalized to *GAPDH*, and presented as mean \pm SE, n=3. SEs range between 6 and 8. * P <0.05 explants vs iPSCs (one-way ANOVA). Panel B shows balanced allelic expression ratio of *KCNQ1-569G* (wild-type) to *KCNQ1-569A* (mutant) in pooled explants derived from two different LQT1 clones (LQT1 Patient II-2, clone a and b). The standard curve plots the Log₂ of the ratio wild-type/mutant (G/A) vs the corresponding delta Ct between the two alleles. LQT1 explants (red circle) result in a delta Ct of 0.22 ± 0.03 , corresponding to an equal allelic expression. Data are presented as mean \pm SE, n=3. Panel C shows similar *KCNQ1* protein expression, as detected by Western blotting, in myocytic explants derived from control and LQT1 iPSCs. Pooled explants from 3 clones per each group were used for total lysate. β -actin is shown as a loading control.



Supplementary Figure 9. Fluorescence Resonance Energy Transfer (FRET) analysis of interaction between wild-type KCNQ1 and R190Q-KCNQ1.

Acceptor photobleaching FRET measurements (panels A-C) in HEK293T cells were performed by co-transfection of constructs coding the cDNA of wild-type KCNQ1 fused to a cyan fluorescent protein (CFP-WT-KCNQ1) or to a yellow fluorescent protein (YFP-WT-KCNQ1), mutated R190Q-KCNQ1 fused to a yellow fluorescent protein (YFP-R190Q-KCNQ1), and β_1 -adrenergic receptor fused to a yellow fluorescent protein (YFP- β_1 -R). Different combinations of the expression plasmids were used as outlined in each panel. The time course of normalized CFP and YFP fluorescence during YFP photobleaching is depicted together with representative images of CFP (upper row) and YFP (lower row) fluorescence at the indicated time points. Panel D shows calculated FRET efficiencies from 6-13 independent measurements. Data are presented as mean \pm SE, * P <0.05 vs CFP-WT-KCNQ1 + YFP-WT-KCNQ1 (two tailed t-test).

Supplementary Figure 10



Supplementary Figure 10. I_{to} and diastolic currents of “ventricular” myocytes from control and LQT1 induced pluripotent stem cells (iPSCs).

Panel A illustrates representative I_{to} current traces (left panel) from a control (black traces) and a LQT1 (red traces) cell and the voltage protocol used for the recordings. Holding potential was at -80 mV and test potentials were from -20 to $+100$ mV with steps of 10 mV lasting 300 msec. Right panel represents standard current-voltage relationship of peak I_{to} currents from control (black squares, 13 cells from three Control-1 clones) and LQT1 (red circles, 13 cells from three LQT1 Patient II-2 clones) myocytes. Panel B shows representative recordings of diastolic currents (left panel) from a control (black traces) and a LQT1 (red traces) myocyte and the corresponding voltage protocol consisting of step of 10 mV increments between -140 and -20 mV (500 msec duration) from a holding potential of -60 mV. This protocol elicits both hyperpolarization-activated (I_h) and inward rectifier (I_{K1}) currents. The right panel shows diastolic current amplitude at the end of the 500 msec pulse plotted as a function of applied voltage for control (black squares, 11 cells from three Control-1 clones) and LQT1 (red circles, 8 cells from three LQT1 Patient II-2 clones) cells.